

Fine, hyperfine and Zeeman structures of levels of $^{123}\text{Sb I}$

Lukasz M. Sobolewski¹, Safa Bouazza², and Jerzy Kwela^{1,a}

¹ Institute of Experimental Physics, University of Gdańsk, ul. Wita Stwosza 57, 80-952 Gdańsk, Poland

² LISM, EA 4695, Université de Reims-Champagne, UFR SEN, BP 1039, 51687 Reims Cedex 2, France

Received 6 July 2015 / Received in final form 29 October 2015

Published online 26 January 2016

© The Author(s) 2016. This article is published with open access at Springerlink.com

Abstract. The hyperfine and Zeeman structures of 14 lines of isotope ^{123}Sb covering the UV-NIR spectral range have been measured. The experimental data have been used in order to reanalyse and revise Sb I energy levels. We named majority of them for the first time since they were previously labelled only by their energy values, without any term designations. In both cases of odd- and even-parity levels we took into consideration up to 7 interacting configurations; the set of fine structure parameters and the leading eigenvector percentages of levels as well as their calculated Landé-factors are given. Semi-empirical hfs parameter values extracted from experimental data were compared with ab initio results computed by the use of Cowan code.

1 Introduction

Natural antimony consists of two stable isotopes ^{121}Sb ($I = 5/2$) and ^{123}Sb ($I = 7/2$), with natural abundance of 57% and 43%, respectively. The large nuclear spins in combination with large nuclear moments ($\mu_I = 3.9796\mu_N$, $Q = -0.36$ barn [1] and $\mu_I = 2.8912\mu_N$, $Q = -0.49$ barn [1,2] for isotopes 121 and 123, respectively) lead to a complex hyperfine structure (hfs) of both isotopes.

Hyperfine structure splitting A and B constants for levels of the ground configuration of Sb I have been obtained in a number of experiments [3–11]. Numerous authors had, at the beginning of Sb I electronic structure studies, looked into the emission spectrum. Later, photoabsorption investigations were preferably used with the flash-pyrolysis technique [12] since the spectrum of atomic antimony is difficult to obtain experimentally because of the tendency for antimony atoms to form dimers and trimers.

The first observation of forbidden lines in antimony was described in reference [3] and the first hfs analysis of the multipole lines of Sb I was performed in reference [4]. In paper [5] the hfs of forbidden lines between levels belonging to the ground configuration of Sb I was studied.

Most of the experimental studies were focused on the hfs of isotope 121, but only a few were dedicated to isotope 123 [6,7]. In addition, the experimental values for ^{123}Sb are inconsistent (see Ref. [13]).

In this paper we report results of observation of hfs and Zeeman structure of 14 emission lines of $^{123}\text{Sb I}$ covering the UV-NIR spectral range ($363.8\div 1074.2$) nm.

The new experimental data have been used in order to reanalyse and revise Sb I energy levels. We found des-

ignations and leading eigenvector percentages for levels belonging to 7 lowest configurations of odd- and even-parities.

2 Experiment

This work is a continuation of our earlier studies of the hfs and Zeeman structures of heavy atoms [13–24]. Measurements were performed to investigate fourteen strongest emission lines in the near visible and infrared region of isotope ^{123}Sb (see Fig. 1).

In the experiment the metallic isotope ^{123}Sb was used. A standard experimental arrangement for observation of hfs and Zeeman structures described in details in a series of our previous papers [13–22] was used. An electrodeless discharge tube powered by a RF generator (55 MHz) was the source of radiation. Helium was used as a buffer gas.

The high-resolution spectral apparatus consisted of a silver-coated Fabry-Pérot étalon (2, 4, 5, 7, 8 and 10 mm spacers were used) and Carl Zeiss Jena PGS-2 grating spectrograph (651.5 grooves/mm, resolution 0.8 nm/mm in the first order) combined with a charge-coupled device (CCD) detector (Hamamatsu model S7032-0906 with head device model C7042).

The Zeeman structure study has been preceded by hyperfine structure observations by the use of various Fabry-Perot spacers. The Zeeman effect studies were performed for transverse direction of observation and separated $\pi(\Delta M = 0)$ and $\sigma(\Delta M = \pm 1)$ components of lines. The light source was placed in a gap of a magnet producing fields up to 2,5 kG. Measurements have been performed for six values of the magnetic field: 1.25, 1.50, 1.75, 2.00, 2.25 and 2.50 kG. The field was measured with an accuracy of 2% by the use of a gaussmeter (Applied Magnetics

^a e-mail: fizjzk@univ.gda.pl

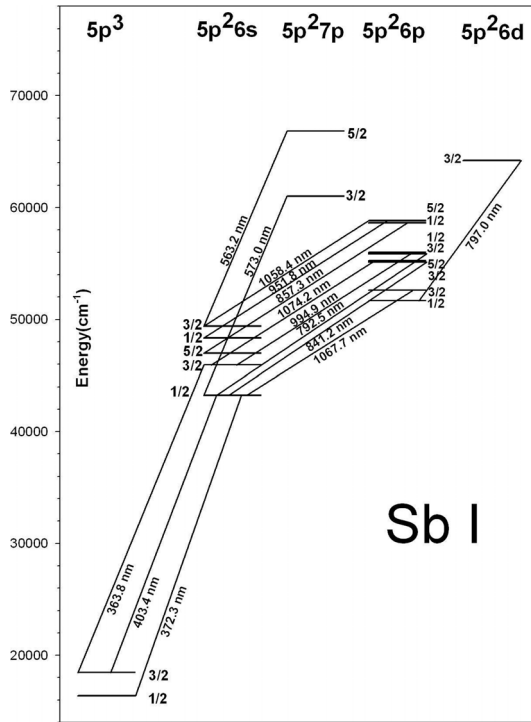


Fig. 1. Energy-level diagram of Sb I with level designation introduced in this work.

Laboratory, model GM1A). Using the strong 605.9 nm ($6p8p^3P_0 \rightarrow 6p7s^3P_1$) line of Pb I, we have calibrated the gaussmeter output to an absolute precision of 1%.

A direct observation of separate hfs Zeeman components is practically unachievable for conditions under which the hfs is barely resolved. What can be observed is an envelope of partially overlapping lines. We assumed that the observed contour is a convolution of Cauchy, Gauss and approximate Airy functions described by the following intensity distribution function [25,26]:

$$I(\nu) = I_0 + C \sum_{i=1}^N \frac{I_0^i}{1 + \alpha_1^2 (\tilde{\nu}_{RL} - \delta\tilde{\nu}_i)^2 + \alpha_2^4 (\tilde{\nu}_{RL} - \delta\tilde{\nu}_i)^4}, \quad (1)$$

where I_0 describes the background noise, C is the scaling factor, N is the number of hfs or hfs Zeeman components, I_0^i is the maximum intensity of the i th component (proportional to the theoretical transition probability), $\tilde{\nu}_{RL}$ is the adjustable parameter in the wave number scale and

$$\delta\tilde{\nu}_i = \delta\tilde{\nu}_i^{up} - \delta\tilde{\nu}_i^{down}, \quad (2)$$

where $\delta\tilde{\nu}_i^{up}$ and $\delta\tilde{\nu}_i^{down}$ are shifts of the energy levels in respect to the position of the centre-gravity for the upper and lower hyperfine structure multiplets, respectively. In the case of hfs studies $\delta\tilde{\nu}_i$ depends on the unknown constants $A(J)$ and $B(J)$. In the analysis of the hf Zeeman structure $\delta\tilde{\nu}_i$ are functions of the unknown parameters A_{down} , A_{up} , B_{down} , B_{up} , g_J^{down} , g_J^{up} .

Details of the computer program for analysis of the hfs-Zeeman structure have been presented in papers [22,23].

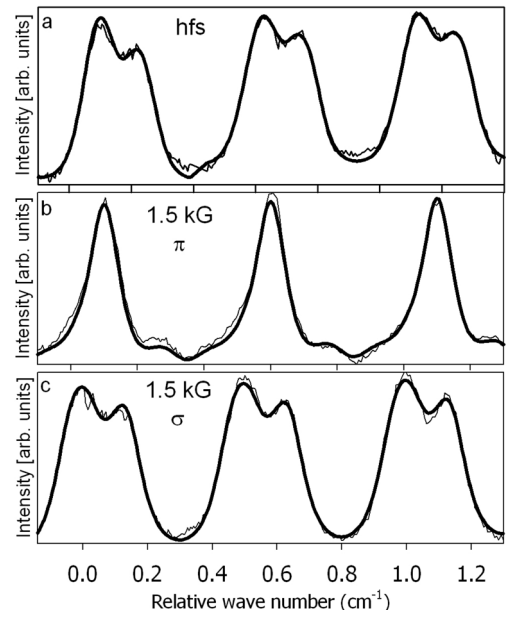


Fig. 2. The recorded hyperfine structure (a) of the 792.5 nm line of $^{123}\text{Sb I}$ obtained with a 10 mm spacer and Zeeman patterns π -view (b) and σ -view (c) at 1.50 kG magnetic field. The thin line represents the experimental trace and the thick line shows the computer-generated contour. The line shape parameters α_1^{-1} and α_2^{-1} are 0.10 and 0.15 cm^{-1} , respectively.

3 Experimental results

Figure 2 presents recorded typical hyperfine and Zeeman structures of the observed lines. Thin lines represent the experimental traces and the thick solid lines are best fits described by formula (1).

Computer simulations yielded values of the hyperfine structure constants A and Landé- g_J factors presented in Table 1. From the spectrum analysis we were unable to determine $B(J)$ values with satisfactory precision, so we decided not to present these data.

The A and g_J constants for all levels listed in this table have been obtained in a similar way to yield agreement between calculated and observed line contours. Each value represents the average of several measurements performed in different experimental conditions. The number of analyzed measurements varied between 14 in the case of 363.8 nm line up to 46 in the case of 1058.5 nm line. Figure 3 shows a histogram of 32 individual measurements of A hfs value for the 43 249.3 cm^{-1} level. Similarly in g_J determinations we used 13 recorded Zeeman spectra in the case of 563.2 nm line and for the line 1058.5 nm the number of spectra was 46. Figure 4 shows a histogram of 44 measurements of Landé- g_J factor for the 52 612.4 cm^{-1} level together with the fitted Gaussian curve.

In Table 1 the atomic structure data are presented together with statistical errors. Numbers in brackets give errors corrected by the Student's t-distribution coefficients. In the case of levels 18 464.2, 43 249.3, 45 945.3, 49 391.1 and 58 835.5 cm^{-1} the A and g_J -constants were obtained with higher reliability as a weighed mean values from observation of more than only one line.

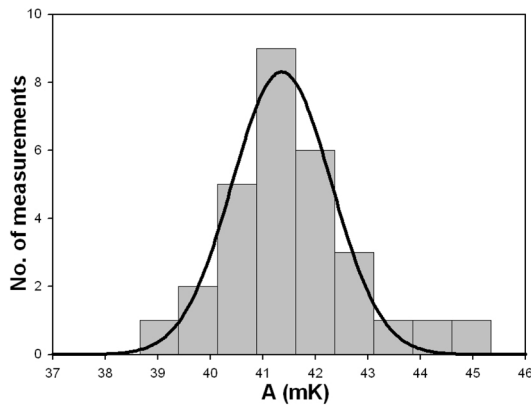


Fig. 3. Histogram for distribution of the experimental data for $43\,249.3\text{ cm}^{-1}$ level for a total of 32 individual measurements of A value ($A = (41.42 \pm 0.09)\text{ mK}$) of 792.5 nm line.

The determined values of hyperfine splitting constant A were found to be consistent with data obtained experimentally for isotope 121 [8]. For a comparison the conversion factor $A_{121}/A_{123} = 1.84661$ [27] should be used.

The Zeeman effect studies delivered 11 new g_J -constants.

4 Fine structure considerations for odd-parity levels

First theoretical studies of the hfs in the antimony atom were performed in references [8,9]. At the same time some fine structure (fs) analyses were achieved [28–30]. The last paper [8], which considers both configurations has added thirty-two new energy levels and revised J values for several energy levels. Nevertheless up to now the odd-parity $5s^25p^2(np + nf)$ configuration levels are not yet well defined since designation terms are missing, as well as calculated Landé-factor values, which are very useful for comparison with experimental data in order to check the validity of level assignments. Furthermore the accuracy of the amplitude of the energy level eigenvector is known to have particularly a strong influence on the determination of the effective mono-electronic hyperfine structure parameters deduced from magnetic dipole A and electric quadrupole B constants, experimentally obtained. For these reasons we propose to extend previous fs studies, using a method successfully tested for atoms: Si I [31], Hf I [32], Zr I [33], and ions: Nb II [34] Ta II [35], V II [36]. This method should find particular application for systems composed of many Rydberg configurations mutually interacting. Here, in the case of odd-parity levels we took into consideration the configuration basis set-up consisted of the following seven configurations: $5s^25p^3$, $5s^25p^26p$, $5s^25p^27p$, $5s^25p^28p$, $5s^25p^29p$, $5s^25p^24f$, $5s^25p^25f$. Although the total number of interaction integrals required for this basis is large, the situation was made tractable by recurring to physically realistic ratios of radial integrals as constraints [31]. For this reason we included in our fitting procedure additional assumptions, selected mainly from

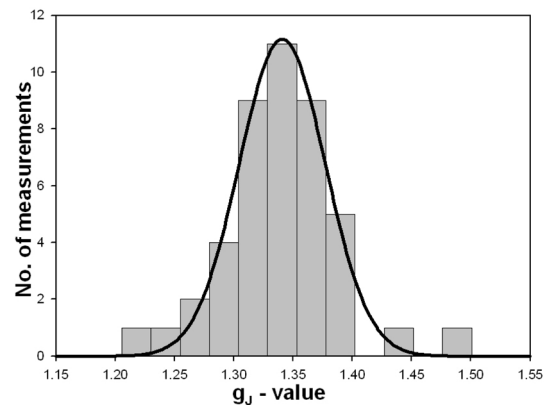


Fig. 4. Histogram for distribution of the experimental data for $52\,612.4\text{ cm}^{-1}$ level for a total of 44 individual measurements of g_J of 1067.7 nm line ($g_J = (1.339 \pm 0.009)$).

Hartree-Fock calculations. The totality of the experimental known odd-parity levels, located up to $90\,000\text{ cm}^{-1}$ were fitted. Thus, the fs least square fitting procedure has been carried out over 68 energy levels listed in reference [8]. With 263 parameters, 16 of which were treated as free, a very good fit has been achieved (standard deviation: 4.8 cm^{-1}).

The coupling scheme used to describe the levels is usually LS coupling, also known as Russell Saunders coupling, L and S designating, respectively, the orbital and spin angular momenta of the state. Entire fs parameter sets of the configurations $5s^25p^3$, and $5s^25p^26p$ were adjusted. With regard to the configurations $5s^25p^27p$, $5s^25p^28p$, $5s^25p^29p$, $5s^25p^24f$, $5s^25p^25f$ only the average energies of configuration centers of gravity E_{av} and the main Slater integrals were fitted. The other parameters are weighed by factor: $0.778 = \frac{28\,170}{36\,199} = \frac{F^2(5p,5p)(fs)}{F^2(5p,5p)(ab\text{ initio})}$, i.e. by the ratio between Slater integrals $F^2(5p, 5p)$ of the main configuration $5p^3$, obtained thanks to the fs study and ab initio calculations. In Table 2, the energy levels, calculated eigenvalues, the resulting LS -percentages of the first and second components of the wavefunctions, and the new LS -term designations are given. In this table, the calculated g_J -factors, deduced from the eigenvector compositions, are compared with experimental ones (when the latter are available) and with ab initio Landé-factor values computed by means of Cowan code [37]. For further extensions of this work we give predicted positions of missing experimental levels up to $89\,000\text{ cm}^{-1}$ as well as their corresponding designation terms and calculated Landé-factor values. Tables 3 and 4 display fitted fs parameter values. Some of the fs parameters, which are expected to be small, have been fixed to zero and are not listed in these two tables.

5 Fine structure considerations for even-parity levels

When we decided to interpret Sb I hfs data of ground configuration levels we, at first, did not insert $5s5p^4$ in

Table 1. Experimental hfs constants A and Landé g_J -factors of ^{123}Sb I levels.

Energy (cm^{-1})	Level [†]	Line (nm)	A (mK)	Landé factor
16 395.4	$5p^3 \ ^2P_{1/2}$	372.3	89.16(0.41)	0.676(0.010)
18 464.2	$5p^3 \ ^2P_{3/2}$	363.8	14.60(0.40)	1.274(0.009)
		403.4	11.60(0.13)	1.280(0.005)
			11.89(0.13)*	1.279(0.005)*
43 249.3	$5p^2 6s^4 P_{1/2}$	372.3	41.31(0.25)	2.328(0.011)
		403.4	42.03(0.50)	2.332(0.009)
		563.2	41.54(0.14)	2.352(0.018)
		792.5	41.59(0.24)	2.345(0.013)
		1067.7	41.24(0.19)	2.357(0.023)
		841.2	41.31(0.38)	2.338(0.011)
		41.42(0.09)*	2.343(0.008)*	
45 945.3	$5p^2 6s^4 P_{3/2}$	363.8	9.52(0.27)	1.722(0.008)
		994.9	9.38(0.23)	1.675(0.006)
		1074.2	9.40(0.18)	1.675(0.015)
		9.42(0.13)*	1.690(0.005)*	
48 332.4	$5p^2 6s^4 P_{5/2}$	951.8	31.59(0.25)	1.536(0.008)
46 991.1	$5p^2 6s^2 P_{1/2}$	857.3	-18.22(0.26)	1.007(0.010)
49 391.1	$5p^2 6s^2 P_{3/2}$	573.0	23.78(0.36)	1.271(0.011)
		1058.5	23.32(0.38)	1.277(0.010)
			23.56(0.27)*	1.274(0.008)*
51 676.4	$5p^2 6p \ ^4D_{1/2}$	797.0	8.18(0.27)	0.711(0.007)
52 612.4	$5p^2 6p \ ^4D_{3/2}$	1067.7	0.84(0.12)	1.339(0.009)
55 134.3	$5p^2 6p \ ^4D_{3/2}$	841.2	1.07(0.21)	1.347(0.028)
55 993.9	$5p^2 6p \ ^4P_{1/2}$	994.9	-19.99(0.41)	2.240(0.017)
55 864.8	$5p^2 6p \ ^2D_{3/2}$	792.5	5.06(0.14)	1.223(0.009)
55 252.1	$5p^2 6p \ ^4D_{5/2}$	1074.2	-2.12(0.16)	1.375(0.009)
58 835.5	$5p^2 6p \ ^2D_{5/2}$	951.8	18.62(0.24)	1.298(0.007)
		1058.5	18.62(0.20)	1.298(0.007)
			18.62(0.16)*	1.298(0.005)*
58 653.0	$5p^2 6p \ ^2P_{1/2}$	857.3	69.38(0.39)	0.978(0.018)
61 000.3	$5p^2 7p \ ^4D_{3/2}$	563.2	0.26(0.09)	1.336(0.010)
64 220.6	$5p^2 6d \ ^2P_{3/2}$	797.0	0.61(0.26)	0.827(0.005)
66 837.6	$5p^2 7p \ ^2D_{5/2}$	573.0	18.45(0.11)	1.279(0.009)

[†] Level designations introduced in this work (largest eigenvalue component).

* Weighted mean value.

the studied configuration basis set-up, thinking that this latter configuration is enough far. Furthermore the paper of Hassini et al. [8] which is the last one devoted to Sb I fine and hyperfine structures confirmed the farness of $5s5p^4$.

Unfortunately when fitting experimental energy levels to determine fine structure (fs) parameters we have noticed that this fit for highest levels is poor. We then

introduced $5s5p^4$ to our studied configuration set and this time a notable improvement has occurred.

Three decades ago one of us (S.B.) performed hyperfine structure measurements of arsenic and was surprised by experimental data obtained in the laboratory: magnetic A factor values of $4s^2 4p^2 5s$ levels were smaller than expected [38]; antimony is placed in the same column as

Table 2. Comparison between observed and calculated energy levels and g_J -factors for odd-parity levels.

Observed energy [8] (cm^{-1})	Calculated eigenvalue (cm^{-1})	Largest eigenvalue component (%)	Next largest component (%)	Theoretical g_J		Observed g_J
				calc.	ab initio*	
$J = 1/2$						
16 395.359	16 294.312	a 99.43 2P	b 0.38 3P; 2P	0.666	0.666	0.676 [†]
51 676.438	51 679.059	b 54.89 3P; 4D	b 17.71 3P; 2S	0.725	0.703	0.711 [†]
54 196.617	54 245.906	b 50.74 3P; 2S	b 35.91 3P; 4D	1.320	1.369	
55 993.859	55 952.148	b 73.06 3P; 4P	b 16.5 3P; 2P	2.244	2.214	2.240 [†]
58 653.012	58 733.266	b 62.54 3P; 2P	b 14.69 3P; 2S	0.947	0.962	0.978 [†]
60 765.293	60 786.535	c 54.13 3P; 4D	c 13.49 3P; 2P	0.666	0.663	
63 606.332	63 636.129	c 39.4 3P; 2S	c 33.88 3P; 4D	1.407	1.538	
64 098.355	64 094.273	d 35.69 3P; 4D	c 15.96 3P; 4P	1.009	0.768	
64 209.430	64 249.219	c 34.67 3P; 4P	c 23.26 3P; 2P	1.415	1.514	
65 479.617	65 479.168	b 70.59 1D; 2P	c 9.06 3P; 2S	0.981	0.968	
65 863.297	65 888.914	f 51.09 3P; 4D	f 19.88 3P; 2P	0.694	0.707	
66 685.102	66 801.648	c 23.33 3P; 2P	c 16.38 3P; 2S	1.038	1.068	
67 192.000	67 109.945	d 44.46 3P; 4P	d 25.22 3P; 4D	1.761	1.806	
67 401.602	67 521.586	d 30.82 3P; 2P	d 28.54 3P; 4P	1.453	1.397	
	68057.656	f 85.7 3P; 4D	g 14.11 1D; 2P	0.093	0.088	
68 945.703	68 926.609	f 36.33 3P; 4D	f 31.65 3P; 2S	1.402	1.518	
69 042.297	69 068.617	f 44.33 3P; 2P	f 44.18 3P; 4P	1.676	1.573	
	69 869.367	d 38.88 3P; 2S	d 29.73 3P; 2P	1.401	1.395	
	70 627.461	h 85.23 3P; 4D	h 14.69 1D; 2P	0.096	0.089	
	71 593.969	f 43.44 3P; 2S	f 26.98 3P; 2P	1.460	1.457	
	73 964.656	c 82.58 1D; 2P	c 6.42 3P; 2S	0.786	0.788	
	74 937.258	b 61.54 1S; 2P	g 23.78 1D; 2P	0.643	0.628	
	75 738.742	g 61.63 1D; 2P	b 25.04 1S; 2P	0.600	0.614	
	77 018.828	d 86.33 1D; 2P	d 7.49 3P; 2S	0.802	0.796	
	78 083.32	h 84.3 1D; 2P	h 14.34 3P; 4D	0.570	0.578	
	78 813.078	f 85.56 1D; 2P	f 8.03 3P; 2S	0.811	0.801	
	84 013.781	c 94.27 1S; 2P	c 2.82 3P; 4D	0.666	0.666	
	87 211.328	d 94.71 1S; 2P	d 2.8 3P; 4D	0.666	0.666	
	89 070.938	f 94.66 1S; 2P	f 2.89 3P; 4D	0.666	0.666	
$J = 3/2$						
0.000	-41.867	a 94.88 4S	a 4.5 2P	1.965	1.973	1.967 ^{††}
8 512.125	8 612.421	a 83.71 2D	a 13.7 2P	0.900	0.888	0.889 ^{††}
18 464.201	18 506.084	a 81.27 2P	a 15.48 2D	1.270	1.275	1.279 [†]
52 612.484	52 581.539	b 43.53 3P; 4D	b 24.68 3P; 4P	1.342	1.341	
55 134.254	55 157.109	b 48.41 3P; 4D	b 18.27 3P; 4S	1.373	1.356	1.347 [†]
55 864.828	55 913.828	b 62.63 3P; 2D	b 20.26 3P; 4S	1.176	1.157	1.223 [†]
58 075.535	57 972.023	b 43.16 3P; 4S	b 41.57 3P; 4P	1.776	1.818	
58 589.512	58 636.996	b 66.27 3P; 2P	b 20.29 1D; 2D	1.229	1.246	
61 000.297	60 972.555	c 30.68 3P; 4D	c 25.13 3P; 4P	1.338	1.341	1.336 [†]
63 798.445	63 797.047	c 31.31 3P; 4S	c 24.65 3P; 4D	1.491	1.441	
63 900.527	63 831.758	c 42.03 3P; 2D	c 26.03 3P; 4D	1.063	1.097	
64 273.855	64 257.734	d 23.85 3P; 2D	d 23 3P; 4D	1.322	1.312	
64 984.586	65 058.238	b 44.84 1D; 2D	c 12.64 3P; 2D	1.067	1.076	
65 565.234	65 575.539	g 62.99 3P; 4F	g 18.34 3P; 2D	0.622	0.622	
65 959.000	65 916.891	b 33.23 1D; 2P	c 17.73 3P; 2P	1.302	1.278	
66 029.789	66 021.359	f 21.74 3P; 4D	f 21.05 3P; 4P	1.324	1.339	
66 541.555	66 483.555	c 42.92 3P; 4S	c 35.72 3P; 4P	1.756	1.780	
66 957.805	67 011.477	d 31.31 3P; 4D	c 17.3 3P; 2P	1.288	1.265	
67 375.227	67 331.57	d 48.92 3P; 2D	d 22.79 3P; 4S	1.297	1.415	

Table 2. Continued.

Observed energy [8] (cm ⁻¹)	Calculated eigenvalue (cm ⁻¹)	Largest eigenvalue component (%)	Next largest component (%)	Theoretical g_J		Observed g_J
				calc.	ab initio*	
67 465.102	67 480.094	d 25.37 3P; 4D	c 18.79 3P; 2P	1.235	1.128	
68 024.688	68 048.766	g 42.83 3P; 2D	h 24.31 3P; 4F	0.719	0.693	
68 070.102	68 052.133	g 51.69 3P; 4D	g 13.04 3P; 2D	1.008	1.084	
	68 137.992	h 27.15 3P; 4F	g 18.56 3P; 4F	0.715	0.662	
68 966.898	68 986.156	f 56.65 3P; 4D	f 20.63 3P; 2P	1.348	1.397	
69 053.797	69 051.445	f 56.23 3P; 2D	f 21.9 3P; 4P	1.243	1.186	
	69 754.797	d 45.92 3P; 4S	d 35.6 3P; 4P	1.777	1.785	
	69 886.039	d 58.57 3P; 2P	d 14.81 1D; 2D	1.220	1.224	
	70 618.562	h 55.05 3P; 2D	h 28.98 3P; 4D	0.987	1.071	
	70 649.562	h 41 3P; 4D	h 29.12 3P; 4F	0.850	0.766	
	71 560.992	f 42.83 3P; 4S	f 38.29 3P; 4P	1.760	1.782	
	71 602.758	f 59.7 3P; 2P	f 14.04 1D; 2D	1.230	1.223	
	73 560.992	c 67.86 1D; 2D	c 12.76 1D; 2P	0.985	1.015	
	74 263.219	c 66.67 1D; 2P	c 12.07 1D; 2D	1.305	1.267	
	75 047.555	b 52.89 1S; 2P	g 32.81 1D; 2P	1.312	1.300	
	75 391.531	g 85.12 1D; 2D	g 5.09 3P; 4F	0.799	0.799	
	75 802.297	g 52.59 1D; 2P	b 34.02 1S; 2P	1.303	1.311	
	76 876.625	d 69.71 1D; 2D	d 13.94 1D; 2P	0.977	1.019	
	77 149.758	d 70.3 1D; 2P	d 12.98 1D; 2D	1.310	1.261	
	77 973.727	h 84.84 1D; 2D	h 5.13 3P; 2D	0.798	0.799	
	78 085.664	h 84.1 1D; 2P	h 7.3 3P; 4D	1.287	1.291	
	78 732.953	f 68.86 1D; 2D	f 15.54 1D; 2P	0.986	1.014	
	78 898.766	f 68.8 1D; 2P	f 14.88 1D; 2D	1.301	1.263	
	84 076.703	c 94.37 1S; 2P	c 1.58 3P; 4P	1.334	1.334	
	87 247.719	d 94.72 1S; 2P	d 1.46 3P; 4P	1.334	1.334	
	89 097.078	f 94.67 1S; 2P	f 1.48 3P; 4P	1.334	1.334	
$J = 5/2$						
9 854.018	10 100.023	a 99.8 2D	b 0.13 3P; 2D	1.200	1.200	1.205 ^{††}
55 252.133	55 246.453	b 72.43 3P; 4D	b 19 3P; 4P	1.401	1.407	1.375 [†]
57 410.340	57 384.125	b 36.5 3P; 4P	b 22.85 3P; 2D	1.358	1.385	
58 835.488	58 837.426	b 53.81 3P; 2D	b 30.93 3P; 4P	1.291	1.276	1.298 [†]
62 462.406	62 463.227	g 41.35 3P; 4G	g 18.05 3P; 2D	0.856	0.856	
63 790.945	63 791.48	c 50.61 3P; 4D	c 18.04 3P; 4P	1.371	1.379	
64 512.391	64 471.82	b 57.39 1D; 2D	b 16.11 1D; 2F	1.214	1.104	
64 878.957	64 884.242	b 63.73 1D; 2F	b 12.13 3P; 2D	1.002	1.093	
64 973.820	64 949.758	h 40.98 3P; 4G	h 17.91 3P; 2D	0.856	0.856	
65 460.148	65 466.785	g 46.83 3P; 4G	g 38.27 3P; 2D	0.908	0.913	
65 568.312	65 571.734	g 34.62 3P; 2F	g 29.63 3P; 4D	1.083	1.078	
66 361.633	66 365.695	c 36.26 3P; 4P	c 28.51 3P; 4D	1.372	1.408	
66 837.570	66 828.227	c 47.47 3P; 2D	c 24.99 3P; 4P	1.293	1.262	1.279 [†]
67 307.000	67 259.797	d 54.4 3P; 4D	d 22.62 3P; 4P	1.389	1.393	
67 994.383	68 008.938	h 45.33 3P; 4G	h 40.12 3P; 2D	0.901	0.914	
68 023.867	68 039.844	h 20.26 3P; 4D	h 17.96 3P; 4F	1.127	1.151	
68 148.219	68 132.734	g 26.88 3P; 4F	g 25.47 3P; 2F	0.968	0.995	
68 157.109	68 141.992	g 26.28 3P; 4D	h 14.68 3P; 2F	1.149	1.086	
69 037.297	68 997.672	f 58.84 3P; 4D	f 24.52 3P; 4P	1.400	1.401	
	69 669.414	d 33.31 3P; 4D	d 30.85 3P; 4P	1.357	1.398	
	69 892.633	d 51.29 3P; 2D	d 32.87 3P; 4P	1.308	1.270	
	70 646.578	h 30.73 3P; 4D	h 28.94 3P; 2F	1.139	1.208	
	70 665.969	h 40 3P; 4F	h 16.96 3P; 4D	1.029	0.964	

Table 2. Continued.

Observed energy [8] (cm^{-1})	Calculated eigenvalue (cm^{-1})	Largest eigenvalue component (%)	Next largest component (%)	Theoretical g_J		Observed g_J
				calc.	ab initio*	
	71 508.406	f 34.14 3P; 4D	f 26.87 3P; 4P	1.338	1.390	
	71 630.258	f 47.57 3P; 2D	f 36.63 3P; 4P	1.325	1.279	
	73 513	c 74.8 1D; 2D	c 11.12 3P; 4P	1.216	1.065	
	73 682.188	c 74.7 1D; 2F	c 10.22 3P; 2D	0.956	1.095	
	75 272.781	g 84.28 1D; 2F	g 5.33 3P; 4F	0.879	0.878	
	75 393.188	g 85.1 1D; 2D	g 7.6 3P; 4D	1.200	1.199	
	76 826.75	d 68.32 1D; 2D	d 16.59 1D; 2F	1.181	1.080	
	76 870.031	d 68.06 1D; 2F	d 16.48 1D; 2D	0.984	1.080	
	77 897.867	h 84.33 1D; 2F	h 5.3 3P; 4F	0.879	0.878	
	77 974.531	h 84.84 1D; 2D	h 7.82 3P; 4D	1.200	1.190	
	78 716.789	f 56.06 1D; 2D	f 28.6 1D; 2F	1.133		
	78 729.586	f 55.91 1D; 2F	f 28.55 1D; 2D	1.034		
$J = 7/2$						
57 555.355	57 506.301	b 85.74 3P; 4D	b 13.41 1D; 2F	1.391	1.395	
62 465.945	62 464.562	g 24.36 3P; 2G	g 22.97 3P; 4D	1.141	1.143	
64 957.230	64 950.938	h 23.44 3P; 2G	h 22.21 3P; 4F	1.142	1.179	
64 978.246	64 966.285	b 81.53 1D; 2F	b 11.82 3P; 4D	1.183	1.144	
65 467.215	65 471.711	g 47.2 3P; 4D	g 29.54 3P; 2G	1.181	1.184	
65 531.000	65 529.789	g 40.45 3P; 4G	g 26.4 3P; 2F	1.024	1.020	
66 405.383	66 382.117	c 83.74 3P; 4D	c 14.79 1D; 2F	1.386	1.390	
67 997.023	68 011.773	h 46.79 3P; 4D	h 31.09 3P; 2G	1.178	1.159	
	68 032.055	h 33.08 3P; 4G	h 22.33 3P; 2F	1.033	1.069	
	68 137.273	g 27.31 3P; 2F	g 24.3 3P; 4F	1.198	1.227	
68 164.055	68 144.484	g 27.67 3P; 4F	g 18.65 3P; 2F	1.087	1.043	
	69 695.461	d 84.79 3P; 4D	d 14.47 1D; 2F	1.388	1.390	
	70 658.297	h 53.08 3P; 2F	h 16.32 3P; 2G	1.060	1.086	
	70 670.648	h 52.81 3P; 4F	h 19.93 3P; 4D	1.228	1.206	
	71 533.18	f 84.59 3P; 4D	f 15.02 1D; 2F	1.386	1.390	
	73 706.133	c 84.75 1D; 2F	c 14.72 3P; 4D	1.186	1.182	
	75 235.273	g 84.11 1D; 2G	g 7.64 3P; 2F	0.920	0.920	
	75 273.195	g 84.25 1D; 2F	g 7.35 3P; 4F	1.160	1.156	
	76 890.367	d 85.08 1D; 2F	d 14.51 3P; 4D	1.185	1.183	
	77 871.938	h 84.19 1D; 2G	h 7.65 3P; 2F	0.919	0.921	
	77 898.383	h 84.26 1D; 2F	h 7.48 3P; 4F	1.160	1.154	
	78 745.922	f 84.76 1D; 2F	f 15.05 3P; 4D	1.186	1.183	
$J = 9/2$						
65 527.793	65 534.508	g 47.8 3P; 4G	g 34.64 3P; 4F	1.218	1.219	
	68 042.992	h 37.89 3P; 4G	h 28.78 3P; 4F	1.217	1.151	
	68 056.703	g 63.79 3P; 2G	g 15.78 3P; 4G	1.102	1.180	
	68 144.547	g 47.36 3P; 4F	g 19.76 3P; 4G	1.244	1.236	
	70 615.656	h 64.03 3P; 2G	h 20.82 3P; 4G	1.094	1.109	
	70 667.602	h 54.31 3P; 4F	h 23.82 3P; 4G	1.247	1.235	
	75 234.539	g 84.1 1D; 2G	g 10.04 3P; 4F	1.136	1.134	
	75 383.852	g 85.27 1D; 2H	g 10.7 3P; 2G	0.941	0.939	
	77 871.938	h 84.21 1D; 2G	h 9.92 3P; 4F	1.136	1.134	
	77 958.906	h 84.94 1D; 2H	h 10.89 3P; 2G	0.942	0.939	
$J = 11/2$						
	68 064.047	g 85.25 3P; 4G	g 14.74 1D; 2H	1.246	1.248	
	70 624.445	h 84.92 3P; 4G	h 15.07 1D; 2H	1.246	1.248	
	75 385.352	g 85.24 1D; 2H	g 14.74 3P; 4G	1.118	1.116	
	77 960.391	h 84.93 1D; 2H	h 15.06 3P; 4G	1.119	1.116	

a: $5p^3$; b: $5p^26p$; c: $5p^27p$; d: $5p^28p$; e: $5p^29p$; f: $5p^24f$; h: $5p^25f$.

† Present work, †† NIST data, * ab initio results obtained by the use of Cowan code.

Table 3. Values of fs-parameters of odd-parity levels of Sb I. The uncertainties given in parentheses are the standard deviations.

Configuration	E_{av}	$F^2(5p, 5p)$	$F^2(5p, np)$ $F^2(5p, nf)$	ξ_{5p}	ξ_{np}	$G^0(5p, np)$	$G^2(5p, np)$	$G^2(5p, nf)$
$5p^3$	10033 (28)	26302 (133)		3270 (44)				
$5p^26p$	60683 (16)	27950 (243)	4159 (127)	3630 (28)	261 ^a	753 ^a	888 ^a	
$5p^27p$	69153 (25)	28404 (247)	1543 (47)	3656 (29)	80 ^a	233 ^a	212 ^a	
$5p^28p$	72404 (43)	28440 (247)	600 (24)	3652 (47)	42 ^a	113 ^a	90 ^a	
$5p^29p$	74203 (22)	28448 (247)	325 (13)	3652 (48)	23 ^a	65 ^a	60 ^a	
$5p^24f$	70750 (21)	28661 (249)	631 (26)	3671 (49)	0 ^a			11 ^a
$5p^25f$	73340 (29)	28786 (250)	395 (16)	3671 (49)	0 ^a			9 ^a

^a Fixed.**Table 4.** Values of configuration interaction parameters for odd-parity levels.

	R^0 (cm ⁻¹)	R^2 (cm ⁻¹)	D^2 (cm ⁻¹)	E^0 (cm ⁻¹)	E^2 (cm ⁻¹)	E^4 (cm ⁻¹)
$5p^3-5p^26p$	587 (70)	1614 (85)				
$5p^3-5p^27p$	260 (31)	1210 (64)				
$5p^3-5p^28p$	245 (30)	969 (51)				
$5p^3-5p^29p$	179 (22)	789 (42)				
$5p^3-5p^24f$		-989 (111)				
$5p^3-5p^25f$		-200 (22)				
$5p^26p-5p^27p$			1825 ^a	485 ^a	500 ^a	
$5p^26p-5p^28p$			980 ^a	330 ^a	352 ^a	
$5p^26p-5p^29p$			700 ^a	238 ^a	250 ^a	
$5p^26p-5p^24f$			912 ^a	-21 ^a		
$5p^26p-5p^25f$			680 ^a	-21 ^a		
$5p^27p-5p^28p$			570 ^a	180 ^a	200 ^a	
$5p^27p-5p^29p$			455 ^a	130 ^a	147 ^a	
$5p^27p-5p^24f$			230 ^a	-7 ^a		
$5p^27p-5p^25f$			100 ^a	-7 ^a		
$5p^28p-5p^29p$			340 ^a	87 ^a	100 ^a	
$5p^28p-5p^24f$			84 ^a	0 ^a		
$5p^28p-5p^25f$			70 ^a	0 ^a		
$5p^29p-5p^24f$			60 ^a	0 ^a		
$5p^29p-5p^25f$			56 ^a	0 ^a		
$5p^24f-5p^25f$			335 ^a		33 ^a	21 ^a

^a Fixed.

arsenic in the periodic table. In the EGAS Conference held in Liege in 1982 Voss and Winkler, Howard and Andrew had been facing the same problem: what is the real impact of close $4s4p^4$ configuration [39], whose levels have very large magnetic structure (because of high influence of Fermi-contact hfs parameter a_{4s}^{10})? Let us point out that a_{ns}^{10} is inversely proportional to the square of principal quantum number n .

Some years later the levels of the latter configuration have been revised and corrected [40–42] and it has been proven that levels of these two configurations mix only very weakly (less than 1%) because they are not as close as previously indicated in reference [39].

Similar situation one of us (J.K.) met performing several years ago calculations of the level structure of the ground $6s^26p^2$ configuration of lead [43]. It was found that

a large impact on the fit of the energy levels had to consider the interaction with distant configuration $6p^4$.

As for many elements, Sb I was first investigated by Meggers and Humphreys [3]. Later Mazzoni and Joshi [28], Joshi et al. [29], Zaidi, Makdisi and Bhatia [12], Beigang and Wynne [30] extended and revised in turn this first analysis. The last but not the least work was done by Hassini et al. [8] who reported 138 levels derived from 617 spectral lines in the range 2536 to 24786 cm⁻¹.

The method applied here for fine and hyperfine structure studies was successfully used previously as regards neutral and singly ionized atoms: Zr I, Hf I, Nb II, Ta II, V II, Ti II [34–36,44,45], gathering the set of their studied configurations in model space when it was possible. In the fs calculations we took into account the basis set-up consisted of the 7 interacting configurations: $5s^25p^26s$,

$5s^25p^27s$, $5s^25p^28s$, $5s5p^4$, $5s^25p^25d$, $5s^25p^26d$ and $5s^25p^27d$. The procedure of fs analysis includes spin-dependent and electrostatic interactions, represented by Slater integrals F^k , G^k and R^k . The spin-orbit integrals ξ_{nd} and ξ_{5p} effect the interactions with distant configurations. We have taken also into account two-body parameters α and β standing for one- and two-electron excitations, respectively. Parametric calculations were performed with the use of the Russel-Saunders (LS) coupling scheme where L and S represent the total angular momentum and the resulting spin quantum numbers for a system of electrons, respectively. The fs least square fitting procedure has been carried out first over all even-parity levels available in literature [3,8,12,28–30], but in the second step we discarded three levels of poor accuracy: $65\,945.699\text{ cm}^{-1}$ ($J = 1/2$), $66\,113.217\text{ cm}^{-1}$ ($J = 3/2$) and $66\,535.190\text{ cm}^{-1}$ ($J = 3/2$). With 53 parameters, 15 of which were treated as free, an excellent fit has been achieved. Tables 5 and 6 contain the values of fs radial parameters obtained thanks to the fitting procedure. When some fs parameters are given without uncertainties this means that to these parameters were given simply ab initio values or were deduced by links with other parameters thanks to ab initio ratio of the corresponding parameters. Let us add that values of some parameters, although predicted by theory but expected to be small in this study were fixed to zero and then are not listed in Tables 5 and 6. In Table 7 the experimental energy levels, calculated eigenvalues, resulting LS -percentage of first and second components of the wave functions, and the corresponding LS -term designations are given. In this table our experimental Landé g_J -factors, as well as those found in literature are compared to those deduced from the eigenvector compositions and those computed by ab initio procedure, recurring to Cowan code [37].

6 Hyperfine interaction

The hyperfine structure of atomic energy levels is caused by the interaction between electrons and the electromagnetic multipole moments of the nucleus.

The hyperfine interaction Hamiltonian can be represented usually by a multipole expansion as follows [46]:

$$H_{hfs} = \sum_{k=1} T^{(k)} M^{(k)} \quad (3)$$

where $T^{(k)}$ and $M^{(k)}$ are spherical tensor operators of rank k in the electronic and nuclear spaces, respectively. In the nonrelativistic framework, the electronic tensor operators in atomic units can be written as:

$$\begin{aligned} T^{(1)} = & \frac{\alpha^2}{2} \sum_{i=1}^N \left\{ 2g_l l^{(1)}(i) r_i^{-3} \right. \\ & - g_s \sqrt{10} \left[C^{(2)}(i) \times s^{(1)}(i) \right]^{(1)} \Big] r_i^{-3} \\ & \left. + g_s \frac{8}{3} \pi \delta(r_i) s^{(1)}(i) \right\} \quad (4) \end{aligned}$$

and

$$T^{(2)} = - \sum_{i=1}^N C^{(2)}(i) r_i^{-3}, \quad (5)$$

where g_l and g_s are the orbital and electron spin g -factors. The three terms in equation (4) are usually called *orbital*, *spin-dipole*, and *Fermi-contact term*, respectively.

Hyperfine interaction couples electronic angular momentum \mathbf{J} and nuclear angular momentum \mathbf{I} to a total angular momentum $\mathbf{F} = \mathbf{I} + \mathbf{J}$. In this representation the diagonal and off-diagonal hyperfine energy corrections are given by:

$$W_{M1}(J, J) = \frac{1}{2} A_J C, \quad (6)$$

$$\begin{aligned} W_{M1}(J, J-1) = & \frac{1}{2} A_{J, J-1} [(K+1)(K-2F) \\ & \times (K-2I)(K-2J+1)]^{1/2}, \quad (7) \end{aligned}$$

$$W_{E2}(J, J) = B_J \frac{3/4C(C+1) - I(I+1)J(J+1)}{2I(2I-1)J(2J-1)}, \quad (8)$$

where $C = F(F+1) - J(J+1) - I(I+1)$ and $K = I+J+F$. The coupling constants are:

$$A_J = \frac{\mu_I}{I} \frac{1}{[J(J+1)(2J+1)]^{1/2}} \langle \gamma J || T^{(1)} || \gamma J \rangle, \quad (9)$$

$$A_{J, J-1} = \frac{\mu_I}{I} \frac{1}{[J(2J-1)(2J+1)]^{1/2}} \langle \gamma J || T^{(1)} || \gamma(J-1) \rangle, \quad (10)$$

$$\begin{aligned} B_J = & 2Q \left[\frac{2J(2J-1)}{(2J+1)(2J+2)(2J+3)} \right]^{1/2} \\ & \times \langle \gamma J || T^{(2)} || \gamma J \rangle. \quad (11) \end{aligned}$$

The nuclear magnetic dipole moment μ_I and nuclear electric quadrupole moment Q are defined through the expectation values of the nuclear tensor operators $M^{(1)}$ and $M^{(2)}$ in the state with the maximum component of the nuclear spin, $M_I = I$:

$$\langle \gamma_I II | M_0^{(1)} | \gamma_I II \rangle = \mu_I, \quad (12)$$

$$\langle \gamma_I II | M_0^{(2)} | \gamma_I II \rangle = \frac{Q}{2}. \quad (13)$$

Together with the nuclear magnetic dipole and electric quadrupole moments the A and B hfs coupling constants yield values of the electronic hyperfine parameters a_l , a_{sd} , a_c and b_q :

$$a_l = \left\langle \gamma LSM_L M_S \left| \sum_{i=1}^N l_0^{(1)}(i) r_i^{-3} \right| \gamma LSM_L M_S \right\rangle, \quad (orbital) \quad (14)$$

Table 5. Values of fs parameters for even-parity levels of Sb I. The uncertainties given in parentheses are the standard deviations.

Config.	$5s^25p^26s$	$5s^25p^27s$	$5s^25p^28s$	$5s5p^4$	Config.	$5s^25p^25d$	$5s^25p^26d$	$5s^25p^27d$
						Fit	Fit	Fit
E_{av}	51756 (26)	66274 (32)	71218 (41)	78138 (203)	E_{av}	62552 (25)	69468 (41)	72610 (59)
$F^2(5p, 5p)$	28170 (120)	28170 (120)	28170 (120)	28170 (120)	$F^2(5p, 5p)$	26988 (226)	26988 (226)	26988 (226)
$G^1(5pns, ns5p)$	2390 (65)	400 (60)	0.00	35052	$F^2(5p, nd)$	6650 (134)	1786 (372)	900 (170)
ξ_{5p}	3560 (19)	3567(19)	3645 (21)	3000	ξ_{5p}	3579 (19)	3631(20)	3642(21)
α	4.5 (2.5)	4.5 (2.5)	4.5 (2.5)	4.5 (2.5)	ξ_{nd}	18	6	3
					α	4.5 (2.5)	4.5 (2.5)	4.5 (2.5)
					$G^1(5p, nd)$	3773 (87)	1519 (182)	650 (103)
					$G^3(5p, nd)$	1652 (147)	927 (239)	420 (97)

Table 6. Values of configuration interaction parameters for even-parity levels.

Interacting configurations	E^1 (cm ⁻¹)	D^2 (cm ⁻¹)	R^1 (cm ⁻¹)	E^3 (cm ⁻¹)
$5s^25p^26s-5s^25p^27s$	890			
$5s^25p^26s-5s^25p^28s$	550			
$5s^25p^26s-5s^25p^25d$	-3206 (113)	-4627 (213)		
$5s^25p^26s-5s^25p^26d$	-780 (160)	-2412 (410)		
$5s^25p^26s-5s^25p^27d$	-560	-1190		
$5s^25p^26s-5s5p^4$			-1978 (150)	
$5s^25p^27s-5s^25p^28s$	261			
$5s^25p^27s-5s^25p^25d$	-750	-1632		
$5s^25p^27s-5s^25p^26d$	-395	-1210		
$5s^25p^27s-5s^25p^27d$	-260	-820		
$5s^25p^27s-5s5p^4$			-750	
$5s^25p^28s-5s^25p^25d$	-500	-1000		
$5s^25p^28s-5s^25p^26d$	-250	-628		
$5s^25p^28s-5s^25p^27d$	-178	-495		
$5s^25p^28s-5s5p^4$			-500	
$5s^25p^25d-5s^25p^26d$	2394(71)	3413 (114)		1795 (108)
$5s^25p^25d-5s^25p^27d$	1750	2160		800
$5s^25p^25d-5s5p^4$			8587 (98)	611
$5s^25p^26d-5s^25p^27d$	948 (81)	1255 (190)		
$5s^25p^26d-5s5p^4$			7305 (165)	
$5s^25p^27d-5s5p^4$			6573 (249)	

$$a_{sd} = \left\langle \gamma LSM_L M_S \left| \sum_{i=1}^N 2C_0^{(2)}(i) s_0(i) r_i^{-3} \right| \gamma LSM_L M_S \right\rangle, \quad (\text{spin-dipole}) \quad (15)$$

$$a_c = \left\langle \gamma LSM_L M_S \left| \sum_{i=1}^N 8\pi\delta^3(r_i) s_0(i) \right| \gamma LSM_L M_S \right\rangle, \quad (\text{Fermi contact}) \quad (16)$$

$$b_q = \left\langle \gamma LSM_L M_S \left| \sum_{i=1}^N 2C_0^{(2)}(i) r_i^{-3} \right| \gamma LSM_L M_S \right\rangle, \quad (\text{electric-quadrupole}) \quad (17)$$

where $M_L = L$ and $M_S = S$.

7 Hyperfine structure considerations for odd-parity levels

Optical hfs investigations started early [6] for this medium heavy element ($Z = 51$). A spectroscopy team from Berlin extended previous investigations using pressure-scanned Fabry-Pérot interferometers [7,9] and some years later, recurring to Fourier-transform spectrometer, the wavelengths of 617 lines have been measured and the hyperfine-structure splitting factors of 77% of these lines were determined by Hassini et al. [8].

Table 8 contains values of fitted hfs parameters with regard to magnetic factor A only. Concerning the hfs analysis, we follow the many-body parameterization method. The radial parameters $a_{nl}^{\kappa k}$, $b_{nl}^{\kappa k}$ have been evaluated by fitting them to experimentally determined hfs constants A and B using the theoretical expressions (Eqs. (4) and (5) of [45] for example). In this aim we used experimental hfs values of Table 1 and some selected ones from paper [8],

Table 7. Comparison between observed and calculated even-parity energy levels and g_J -factors.

J	Observed energy [8] (cm^{-1})	Calculated eigenvalue (cm^{-1})	Largest eigenvalue component (%)	Next largest component (%)	Theoretical g_J		Experimental g_J	
					calc.	ab initio*	this work	others [†]
0.5	43 249.336	43 229.395	a 80.94 3P4P	a 13.64 3P2P	2.356	2.350	2.343	2.332
0.5	46 991.059	47 027.316	a 79.57 3P2P	a 15.58 3P4P	0.984	0.990	1.007	1.004
0.5	56 698.609	56 642.598	d 36.68 3P4P	d 32.63 3P4D	1.526	1.396		
0.5	57 597.203	57 678.273	d 21.65 3P4D	d 21.14 3P2P	1.471	1.479		
0.5	58 132.656	58 150.008	b 55.60 3P4P	b 21.89 3P2P	1.914	1.823		
0.5	59 737.625	59 735.121	d 50.66 3P2P	d 32.04 3P4D	0.609	0.851		
0.5	61 386.508	61 290.504	b 67.32 3P2P	b 24.47 3P4P	1.166	1.132		
0.5	62 960.316	62 985.121	c 62.03 3P4P	c 30.62 3P2P	1.994	2.043		
0.5	63 825.758	63 757.918	e 34.15 3P4D	e 20.16 3P4P	1.411	0.846		
0.5	64 769.176	64 731.531	e 41.41 3P4D	g 14.95 3P4P	1.257	1.904		
0.5	65 654.406	65 624.992	a 73.74 1S2S	d 9.19 1D2S	2.002	1.852		
0.5	66 009.711	65 986.711	c 62.13 3P2P	c 31.98 3P4P	1.325	1.264		
0.5	66 353.859	66 299.922	e 43.20 3P2P	d 22.01 1D2P	0.699	0.739		
0.5	67 427.023	67 382.953	d 61.27 3P4D	f 15.50 3P2P	0.625	0.454		
0.5		68 451.250	d 42.80 1D2P	e 14.54 3P2P	0.864	0.670		
0.5		68 670.328	d 23.02 3P4P	f 22.54 3P4P	1.941	2.106		
0.5		69 086.992	d 62.79 1D2S	a 13.99 1S2S	1.942	2.161		
0.5		70 040.359	f 60.08 3P2P	f 15.79 3P4D	0.625	0.616		
1.5	45 945.340	45 942.695	a 92.52 3P4P	a 6.76 3P2P	1.705	1.705	1.690	1.713
1.5	49 391.133	49 347.133	a 67.45 3P2P	a 16.64 1D2D	1.253	1.265	1.274	1.277
1.5	53 527.957	53 489.625	d 58.53 3P4F	d 10.87 3P4D	0.719	0.740		
1.5	55 232.965	55 247.754	a 46.83 1D2D	d 13.38 3P2P	1.051	1.015		0.991
1.5	56 151.801	56 196.727	d 28.20 3P4P	a 25.65 1D2D	1.224	1.250		1.302
1.5	56 733.160	56 655.125	d 49.60 3P2P	d 12.24 3P4P	1.285	1.256		1.311
1.5	58 746.355	58 773.828	d 70.99 3P4D	g 6.79 3P4P	1.218	1.226		
1.5	60 580.898	60 544.223	d 27.83 3P2D	e 22.37 3P4F	0.840	0.854		
1.5	60 964.672	60 981.961	b 84.58 3P4P	b 13.02 3P2P	1.678	1.166		
1.5	61 808.699	61 867.086	d 32.89 3P2D	e 19.65 3P4F	0.881	0.838		
1.5	63 193.031	63 222.086	e 22.51 3P4F	e 17.39 3P4P	1.294	1.147		
1.5	63 649.461	63 667.332	b 61.30 3P2P	b 13.48 1D2D	1.301	1.315		
1.5	64 220.605	64 257.441	f 29.04 3P4F	e 18.80 3P2P	0.878	0.884	0.827	
1.5	64 432.395	64 586.117	d 20.60 1D2D	e 19.61 3P2P	0.970	0.884		
1.5	64 843.422	64 862.508	d 35.62 1D2D	e 11.04 3P2P	0.999	1.126		
1.5	65 143.602	65 231.434	e 56.73 3P4D	e 10.34 3P2D	1.177	1.312		
1.5	66 023.102	66 022.602	c 81.48 3P4P	c 16.76 3P2P	1.661	1.627		
1.5		66 952.930	e 34.07 3P2D	f 9.28 3P2D	0.960	0.949		
1.5		67 253.469	f 32.38 3P4F	f 17.34 3P2P	1.133	1.101		
1.5		67 857.016	f 22.64 3P2P	e 16.74 3P2D	1.135	1.182		
1.5		68 411.617	c 47.77 3P2P	d 16.49 1D2P	1.301	1.247		
1.5		68 776.828	f 36.47 3P4D	e 18.80 3P4P	1.325	1.307		
1.5		69 205.336	d 53.86 1D2P	c 14.44 3P2P	1.309	1.419		
1.5		69 943.539	f 36.96 3P2D	f 20.12 3P2P	0.947	0.948		
1.5		70 895.719	b 69.60 1D2D	b 11.38 3P2P	0.933	0.914		
1.5		71 464.836	f 41.94 3P4P	g 23.27 3P4P	1.566	1.622		
1.5		72 628.797	e 50.38 1D2D	d 10.20 1D2D	0.910	0.882		

Table 7. Continued.

J	Observed energy [8] (cm^{-1})	Calculated eigenvalue (cm^{-1})	Largest eigenvalue component (%)	Next largest component (%)	Theoretical g_J		Experimental g_J	
					calc.	ab initio*	this work	others [†]
1.5		74 514.812	e 75.74 1D2P	e 11.05 3P4P	1.364	1.354		
1.5		75 728.305	c 82.77 1D2D	c 12.70 3P2P	0.899	0.901		
2.5	48 332.426	48 328.031	a 86.49 3P4P	a 12.84 1D2D	1.549	1.553	1.536	1.547
2.5	53 442.969	53 342.336	d 38.77 3P4P	g 16.25 3P4P	1.417	1.432		
2.5	55 120.941	55 181.488	d 42.71 3P4F	a 21.50 1D2D	1.205	1.196		
2.5	55 728.266	55 759.969	a 57.57 1D2D	d 10.85 3P4F	1.262	1.257		1.277
2.5	57 287.051	57 342.688	d 58.15 3P2F	d 19.11 3P4F	0.935	0.946		
2.5	58 862.891	58 885.988	d 56.82 3P4D	d 12.14 3P2F	1.287	1.263		
2.5	60 404.477	60 502.965	d 24.08 3P2D	d 13.06 1D2F	1.218	1.168		
2.5	61 631.066	61 642.484	d 31.54 3P2D	d 12.50 1D2D	1.284	1.282		
2.5	62 501.727	62 436.797	e 24.87 3P4F	g 16.08 3P4P	1.274	1.330		
2.5	63 516.281	63 541.152	b 81.89 3P4P	b 14.09 1D2D	1.537	1.494		
2.5	64 213.707	64 220.074	e 18.10 3P4F	f 13.23 3P4F	1.187	1.136		
2.5	64 513.703	64 624.145	e 28.60 3P2F	d 21.96 1D2D	1.124	1.185		
2.5	65 243.250	65 160.602	e 28.18 3P2F	d 18.64 1D2D	1.133	1.095		
2.5		65 543.594	e 24.02 3P4F	e 20.79 3P4D	1.206	1.271		
2.5		66 472.805	e 26.81 3P2D	d 25.66 1D2F	1.087	1.100		
2.5		66 997.102	e 21.28 3P4D	f 19.78 3P4F	1.300	1.267		
2.5		67 884.172	f 31.84 3P2F	f 23.30 3P4F	1.028	1.028		
2.5		68 385.461	e 25.03 3P2D	d 11.22 1D2F	1.168	1.430		
2.5		68 586.609	c 74.88 3P4P	c 13.06 1D2D	1.499	1.201		
2.5		68 841.891	f 24.37 3P4D	f 12.99 3P4F	1.273	1.332		
2.5		70 232.789	f 29.35 3P2D	f 16.57 3P4D	1.179	1.183		
2.5		70 575.656	f 29.06 3P4P	f 17.58 3P2D	1.361	1.407		
2.5		70 749.977	b 73.11 1D2D	b 12.22 3P4P	1.257	1.259		
2.5		72 783.438	e 45.18 1D2D	g 8.16 1D2D	1.250	1.224		
3.5	56 528.133	56 573.910	d 72.34 3P4F	d 19.73 3P4D	1.270	1.278		
3.5	58 944.148	58 919.750	d 40.56 3P4D	d 17.84 3P4F	1.266	1.289		
3.5	61 125.742	61 035.402	d 59.99 3P2F	d 25.52 3P4D	1.188	1.174		
3.5	64 120.879	64 112.078	e 46.30 3P4F	e 30.28 3P4D	1.284	1.276		
3.5	65 403.797	65 383.625	d 55.01 1D2F	d 14.11 1D2G	1.152	1.135		
3.5		66 622.445	d 48.26 1D2G	e 17.58 3P2F	1.013	1.039		
3.5	66 743.125	66 787.117	e 47.80 3P4D	e 23.56 3P4F	1.281	1.261		
3.5	67 358.203	67 363.070	f 35.59 3P4F	f 22.61 3P4D	1.238	1.266		
3.5	68 079.695	68 003.930	e 31.68 3P2F	f 14.63 3P4F	1.175	1.164		
3.5		69 963.523	f 38.62 3P4F	f 38.59 3P4D	1.280	1.287		
3.5		70 400.375	f 64.14 3P2F	f 13.94 3P4D	1.152	1.153		
4.5		58 572.621	d 86.09 3P4F	d 11.07 1D2G	1.309	1.312		
4.5	66 428.102	66 346.453	d 52.47 1D2G	e 40.22 3P4F	1.208	1.163		
4.5		66 820.094	e 41.45 3P4F	d 35.78 1D2G	1.229	1.276		
4.5		69 965.961	f 82.58 3P4F	f 15.68 1D2G	1.299	1.304		

a: $5p^26s$; b: $5p^27s$; c: $5p^28s$; d: $5p^25d$; e: $5p^26d$; f: $5p^27d$; g: $5s5p^4$.

[†] Data from NIST, * ab initio results obtained by the use of Cowan code.

Table 8. The fitted hfs parameters for the magnetic dipole interaction for odd-parity levels; in parentheses are the standard deviations.

Config.	a_{5p}^{01} (mK)	a_{5p}^{12} (mK)	a_{5p}^{10} (mK)	a_{np}^{01} (mK)	a_{np}^{12} (mK)
$5s^25p^3$	27.51 (0.07)	37.41 (0.09)	-6.88 (0.02)		
$5s^25p^26p$	32.78 (0.14)	44.58 (0.19)	-6.01 (0.45)	2.42(0.08)	3.28 (0.11)
$5s^25p^27p$	33.43 (0.14)	45.47 (0.19)	-6.01 (0.45)	0.80 (0.03)	1.08 (0.04)
$5s^25p^28p$	33.76 (0.14)	45.91 (0.19)	-6.01 (0.45)	0.37 (0.01)	0.41 (0.02)
$5s^25p^29p$	34.09 (0.14)	46.36 (0.19)	-6.01 (0.45)	0.08 (0.07)	0.09(0.09)
$5s^25p^24f$	34.09 (0.14)	46.36 (0.19)	-0.98 (0.46)	0.00	0.00
$5s^25p^25f$	34.09 (0.14)	46.36 (0.19)	-1.27 (0.66)	0.00	0.00

Table 9. The calculated parameters for the magnetic dipole interaction for odd-parity levels.

Config.	$\langle r^{-3} \rangle_{5p}$ (a.u.)	a_{5p}^{01} (mK)	a_{5p}^{12} (mK)	$\langle r^{-3} \rangle_{np}$ (a.u.)	a_{np}^{01} (mK)	a_{np}^{12} (mK)
				$\langle r^{-3} \rangle_{nf}$ (a.u.)	a_{nf}^{01} (mK)	a_{nf}^{12} (mK)
$5s^25p^3$	10.52	27.63	37.58			
$5s^25p^26p$	12.55	32.96	44.83	0.78	2.05	2.79
$5s^25p^27p$	12.59	33.07	44.98	0.26	0.68	0.92
$5s^25p^28p$	12.62	33.12	45.04	0.12	0.32	0.44
$5s^25p^29p$	12.61	33.12	45.04	0.07	0.18	0.24
$5s^25p^24f$	12.62	33.15	45.08	4.60e-4	0.00	0.00
$5s^25p^25f$	12.62	33.15	45.08	2.40e-4	0.00	0.00

which seem be not affected by false fs designation and not questionable about their accuracy. Since these latter values were measured for ^{121}Sb isotope we converted them, introducing the ratio: $A_{121}/A_{123} = g_I 121/g_I 123 = 1.84661$ [27] confirmed in a precision atomic beam magnetic resonance experiment [11]. It should be noted that the converted data neglect possible effects of hfs-anomalies different for different levels [47]; such an effect was observed for the ground level of antimony [11,27].

The number of experimental hfs A -values is larger than the number of many-body parameters required by theory and then no additional assumptions had to be included in our hfs fitting procedure. To check the validity of the hfs many-body parameter values for p -electrons one can use, for instance, the well-established relations (in mK): $a_{nl}^{\kappa k} = 2\mu_0\mu_B\mu_I\langle r^{-3} \rangle_{nl}^{\kappa k}/4\pi I = 3.180g_I\langle r^{-3} \rangle_{nl}^{\kappa k}$ where the computed expectation values $\langle r^{-3} \rangle_{nl}^{\kappa k}$ are given in Table 9 thanks to Cowan code. Here we have $g_I = \mu_I/I = 2.8912/3.5$.

Regarding f -electrons there is no hfs splitting since Sb I spin-orbit constants of $4f$ and $5f$ are equal to zero.

We can compare the calculated hfs many-body parameter values of Table 9 with those from Table 6 deduced by fitting them to experimentally determined hfs constants A of Table 10. One can notice that the agreement is very satisfactory. Regarding the B-factor, the dispersion of published experimental values and particularly their signs, due to different precisions of the applied methods, is so big that we have decided not to look into this problem now. Moreover, in paper [8] the B-factor contribution for many levels is out right neglected.

8 Hyperfine structure considerations for even-parity levels

For hfs analysis we follow the many-body parameterization method described in reference [48] which allows us to take advantage of similarities between configuration interaction effects observed independently in spin-orbit and hyperfine splitting.

Table 11 contains values of fitted hfs parameters with regard to magnetic factor A only. The fitted values were compared with our experimental data and data from paper [8] obtained for isotope ^{121}Sb and converted for isotope 123. The converted data neglects the A -hfs anomalies which can vary between different levels [11,27,47].

The radial parameters $a_{nl}^{\kappa k}$ and $b_{nl}^{\kappa k}$ have been evaluated by fitting them to experimentally determined hfs constants A and B using the theoretical expressions (Eqs. (4) and (5) of [45] for example). A good fit, with a root mean square deviation of 0.55 mK was obtained for selected accurate hfs values given in reference [8] gathered with our data given in Table 1. Table 12 contains the values of fitted hfs parameters quoted with their uncertainties with regard to magnetic dipole interaction only: the hfs parameters relative to electric factor B present more uncertainties because some experimental values given in literature seem doubtful, particularly their sign. In order to check validity of these fitted parameters we have compared some of them to ab initio values obtained by means of Cowan code [37]. For instance one can use the well-established relation

$$a_{nl}^{\kappa k} (\text{mK}) = \frac{2\mu_0\mu_B\mu_I\langle r^{-3} \rangle_{nl}^{\kappa k}}{4\pi I} = 3.18g_I\langle r^{-3} \rangle_{nl}^{\kappa k}.$$

Table 10. Comparison between experimental and calculated A hfs magnetic factors for odd-parity levels of ^{123}Sb .

Energy level cm^{-1}	$A^{Exp.}(\text{mK})$		$A(\text{mK})$ calc	Energy level cm^{-1}	$A^{Exp.}(\text{mK})$		$A(\text{mK})$ calc	Energy level cm^{-1}	$A^{Exp.}(\text{mK})$		$A(\text{mK})$ calc
	this work	other*			this work	other*			this work	other*	
$J = 1/2$				67 465.10			10.03	71 508.41			23.08
16 395.35	89.16	88.65	89.05	68 024.68			-21.49	71 630.26			18.17
51 676.43	8.18	8.06	8.10	68 070.10			1.44	73 513.00			15.42
54 196.61		-15.65	-14.94	68 137.99			3.60	73 682.19			19.62
55 993.85	-19.99	-19.66	-20.07	68 966.89			-3.57	75 272.78			6.70
58 653.01	69.38	69.05	69.34	69 053.79			-1.97	75 393.19			0.35
60 765.29		7.31	7.20	69 754.80			27.52	76 826.75			16.44
63 606.33		-12.89	-12.45	69 886.04			27.39	76 870.03			18.84
64 098.35			1.41	70 618.56			-22.46	77 897.87			6.51
64 209.43			-3.91	70 649.56			3.40	77 974.53			0.57
65 479.61			47.98	71 560.99			25.31	78 716.79			17.88
65 863.29			1.40	71 602.76			31.42	78 729.59			17.42
66 685.10			51.26	73 560.99			26.04	$J = 7/2$			
67 192.00			-7.01	74 263.22			19.96	57 555.35		15.98	16.23
67 401.60			10.79	75 047.56			-6.64	62 465.94		-0.38	0.14
68 057.66			-39.92	75 391.53			0.02	64 957.23		11.70	7.31
68 945.70			-8.09	75 802.30			-7.22	64 978.24		1.52	6.99
69 042.29			0.87	76 876.63			27.28	65 467.21		-0.27	-0.25
69 869.37			60.38	77 149.76			20.97	65 531.00		-1.95	-1.22
70 627.46			-40.23	77 973.73			-1.23	66 405.38		11.81	16.17
71 593.97			60.38	78 085.66			-15.38	67 997.02		-0.70	1.82
73 964.66			51.11	78 732.95			27.84	68 032.06			2.72
74 937.26			-6.39	78 898.77			21.27	68 137.27			2.60
75 738.74			-18.83	84 076.70			0.12	68 164.05			8.79
77 018.83			50.35	87 247.72			0.15	69 695.46			16.39
78 083.32			-33.06	89 097.08			-0.05	70 658.30			9.02
78 813.08			50.41	$J = 5/2$				70 670.65			8.92
84 013.78			2.80	9 854.01		26.54	26.69	71 533.18			16.56
87 211.33			0.61	55 252.13	-2.12	-2.27	-2.20	73 706.13			13.92
89 070.94			0.06	57 410.34		22.53	22.32	75 235.27			9.32
$J = 3/2$				58 835.48	18.62	18.79	18.55	75 273.20			5.67
0.00		-5.52	-4.92	62 462.40			0.04	76 890.37			14.12
8 512.12		10.21	10.79	63 790.94		-0.43	0.50	77 971.94			9.26
18 464.20	11.89	12.30	11.85	64 512.39		14.08	13.54	77 898.38			5.74
52 612.48	0.84	0.81	1.38	64 878.95		17.11	17.12	78 745.92			14.09
55 134.25	1.07	1.19	1.41	64 973.82		-0.11	0.03	$J = 9/2$			
55 864.82	5.06	5.20	5.36	65 460.14		-0.70	-0.12	65 527.79		-1.03	-0.89
58 075.53		27.51	27.57	65 568.31		1.19	0.80	68 042.99			12.63
58 589.51		19.12	19.15	66 361.63		11.00	22.72	68 056.70			1.07
61 000.29	0.26	0.38	0.36	66 837.57	18.45	17.98	17.42	68 144.55			7.36
63 798.44		-3.25	-4.02	67 307.00			-1.84	70 615.66			12.59
63 900.52		5.09	5.10	67 994.38		-0.97	0.25	70 667.60			9.67
64 273.85			1.45	68 023.86			-0.99	75 234.54			7.63
64 984.58		16.03	15.78	68 148.21			5.98	75 383.85			11.07
65 565.23		1.90	1.38	68 157.10			5.22	77 871.94			7.54
65 959.00			19.66	69 037.29			-2.96	$J = 11/2$			
66 029.78			3.01	69 669.41			22.95	68 064.05			11.01
66 541.55			28.36	69 892.63			17.85	70 624.45			11.05
66 957.80			8.58	70 646.58			1.15	75 385.35			9.11
67 375.22			-0.64	70 665.97			8.08	77 960.39			9.07

* Data converted from experimental results for isotope ^{121}Sb [8] using the ratio $\frac{A_{121}}{A_{123}} = \frac{g_I(121)}{g_I(123)} = 1.84661$ [27].

Table 11. Comparison of experimental and calculated A hfs for even-parity levels of ^{123}Sb .

J	Energy levels (cm^{-1})	$A^{Exp.}$ (mK)		A^{Calc} (mK)	J	Energy levels (cm^{-1})	$A^{Exp.}$		A^{Calc} (mK)
		this work	other*				this work	other*	
0.5	43 249.33	41.42	41.05	41.40	1.5	71 464.83	–	–	31.12
0.5	46 991.05	–18.22	–18.41	–18.77	1.5	72 628.79	–	–	7.64
0.5	56 698.60		9.53	10.21	1.5	74 514.81	–	–	8.64
0.5	57 597.20		81.61	81.32	1.5	75 728.30	–	–	25.19
0.5	58 132.65		49.12	20.98	2.5	48 332.42	31.59	31.52	30.79
0.5	59 737.62		–15.00	–10.97	2.5	53 442.96		20.63	16.91
0.5	61 386.50		–11.21	–8.37	2.5	55 120.94		16.84	15.19
0.5	62 960.31		4.98	6.17	2.5	55 728.26		27.02	23.47
0.5	63 825.75		20.36	14.24	2.5	57 287.05		15.60	15.76
0.5	64 769.17		83.02	98.19	2.5	58 862.89		22.53	21.69
0.5	65 654.40		–	48.86	2.5	60 404.47		6.23	7.03
0.5	66 009.71		–13.21	–10.08	2.5	61 631.06		4.55	6.66
0.5	66 353.85		–	–24.36	2.5	62 501.72		17.87	18.13
0.5	67 427.02		–	1.92	2.5	63 516.28		24.64	23.04
0.5	68 451.25		–	13.94	2.5	64 213.70		–	0.83
0.5	68 670.32		–	53.24	2.5	64 513.70		13.65	10.58
0.5	69 086.99		–	33.27	2.5	65 243.25		19.71	16.80
0.5	70 040.35		–	–21.10	2.5	65 543.59		–	18.24
0.5	72 125.93		–	105.09	2.5	66 472.80		–	3.85
1.5	45 945.34	9.42	9.37	9.45	2.5	66 997.10		–	7.62
1.5	49 391.13	23.56	23.50	22.59	2.5	67 884.17		–	2.26
1.5	53 527.95		5.31	4.40	2.5	68 385.46		–	13.01
1.5	55 232.96		5.69	9.23	2.5	68 586.60		–	22.00
1.5	56 151.80		16.52	14.89	2.5	68 841.89		–	21.11
1.5	56 733.16		8.83	3.68	2.5	70 232.78		–	18.36
1.5	58 746.35		26.21	25.04	2.5	70 575.65		–	15.76
1.5	60 580.89		8.29	7.10	2.5	70 749.97		–	18.41
1.5	60 964.67		–1.62	–2.67	2.5	72 783.43		–	19.19
1.5	61 808.69		14.95	14.67	3.5	56 528.13		–	–0.48
1.5	63 193.03		11.86	12.80	3.5	58 944.14		11.86	12.32
1.5	63 649.46		26.70	29.64	3.5	61 125.74		12.35	12.58
1.5	64 220.60	0.61	2.27	1.56	3.5	64 120.87		–1.25	–1.74
1.5	64 432.39		–3.25	–0.45	3.5	65 403.79		–	10.07
1.5	64 843.42		–	6.17	3.5	66 622.44		–	13.71
1.5	65 143.60		–	24.83	3.5	66 743.12		11.43	12.58
1.5	66 023.10		–	–1.77	3.5	67 358.20		–	3.12
1.5	66 113.21		–	13.87	3.5	68 079.69		–	8.53
1.5	67 253.46		–	–0.57	3.5	69 963.52		–	14.62
1.5	67 857.01		–	4.08	3.5	70 400.37		–	14.21
1.5	68 411.61		–	23.19	4.5	58 572.62		–	11.51
1.5	68 776.82		–	32.39	4.5	66 428.10		10.83	11.78
1.5	69 205.33		–	14.87	4.5	66 820.09		–	11.32
1.5	69 943.53		–	15.35	4.5	69 965.96		–	12.71

* Data converted from experimental results for isotope ^{121}Sb [8] using the ratio $\frac{A_{121}}{A_{123}} = \frac{g_I(121)}{g_I(123)} = 1.84661$ [27].

Table 12. The fitted hfs parameters for the magnetic dipole interaction for even-parity levels. The uncertainties given in parentheses are the standard deviations.

Configuration	a_{5p}^{01} (mK)	a_{5p}^{12} (mK)	a_{5p}^{10} (mK)	a_{ns}^{10} (mK)	a_{nd}^{01} (mK)	a_{nd}^{12} (mK)
$5s^2 5p^2 6s$	30.16 (0.32)	40.73 (0.44)	-1.02 (0.55)	49.09 (0.59)		
$5s^2 5p^2 7s$	30.76 (0.32)	41.54 (0.45)	-1.02 (0.55)	14.30 (0.15)		
$5s^2 5p^2 8s$	30.76 (0.32)	41.54 (0.45)	-1.02 (0.55)	7.45 (0.09)		
$5s 5p^4$	26.15 (0.28)	35.31 (0.38)	-0.83 (0.45)	472.69 (4.95)		
$5s^2 5p^2 5d$	30.34 (0.32)	40.97 (0.44)	-1.02 (0.55)		0.21 (0.03)	0.20 (0.03)
$5s^2 5p^2 6d$	31.97 (0.34)	43.17 (0.47)	-1.02 (0.55)		0.00	0.00
$5s^2 5p^2 7d$	31.97 (0.34)	43.17 (0.47)	-1.02 (0.55)		0.00	0.00

Table 13. The calculated parameters for the magnetic dipole interaction for even-parity levels.

Configuration	$\langle r^{-3} \rangle_{np}$ (a.u.)	$\langle r^{-3} \rangle_{nd}$ (a.u.)	ξ_{np}	ξ_{nd}	a_{5p}^{01} (mK)	a_{5p}^{12} (mK)	a_{nd}^{01} (mK)	a_{nd}^{12} (mK)
$5p^2 6s$	12.29		3421		29.63	40.01		
$5p^2 7s$	12.54		3491		30.12	40.68		
$5p^2 8s$	12.59		3504		30.22	40.81		
$5s 5p^4$	10.66		2967		25.69	34.64		
$5p^2 5d$	12.36	0.09	3439	18.9	29.80	40.24	0.20	0.20
$5p^2 6d$	12.54	0.03	3489	7.0	30.24	40.84	0.07	0.07
$5p^2 7d$	12.58	0.02	3502	3.5	30.35	40.99	0.04	0.04

Table 14. Pseudo-relativistic Hartree-Fock estimates of $4\pi|\Psi(0)|^2$ (in a.u.) for studied in the present paper even-parity configurations, using the PSUHFR code [51].

Configuration	$5s 5p^4$	$5p^2 6s$	$5p^2 7s$	$5p^2 8s$
1s	944 880.00	94 4886.00	944 883.00	944 880.00
2s	104 264.00	104 267.00	104 268.00	104 268.00
3s	20 225.00	20 230.00	20 229.00	20 229.00
4s	3 906.00	3 917.00	3 917.00	3 917.00
5s	414.38	429.00	429.00	429.00
6s		27.14		
7s			8.05	
8s				3.52
Total <i>s</i> -electron density ^a	2 146 963.00	2 147 485.00	2 147 462.00	2 147 449.00

^a Totals are contributions from all *s*-orbitals weighted by their occupation number.

To give it experimental significance we have to weight it by the ratio of spin-orbit constants obtained thanks to fs study and ab initio calculations, i.e. to multiply it by $\xi_{nl}(fs)/\xi_{nl}$ (ab initio) as we did for instance in previous work [35]. Using the expectation values of Table 13, knowing that the magnetic dipole moment of ^{123}Sb is equal to $2.8912 \mu_n$ one gets the a_{nl}^{01} and a_{nl}^{12} values of Table 13 which are very close to experimental ones (Tab. 12). We used $a_{nl}^{12} = 1.35a_{nl}^{01}$ for *p*-electron and $a_{nl}^{12} = 0.97a_{nl}^{01}$ for *d*-electron keeping the ratio obtained experimentally.

To test exactness of the most influential hfs parameters a_{ns}^{10} of $5p^2 ns$ and $5s 5p^4$ configurations it is interesting to compare the corresponding ratio a_{ns}^{10}/μ_I for Sb I, to those of its neighbours Sn I and Te I and usually a_{ns}^{10}/μ_I (Sn I) < a_{ns}^{10}/μ_I (Sb I) < a_{ns}^{10}/μ_I (Te I). Unfortunately some of these parameter values are not available in literature. There is one solution left: to

use $a_{ns}^{10}(\text{mK}) = 3.18g_I \langle r^{-3} \rangle ns = 2.12g_I 4\pi|\psi(0)|^2$. We give in Table 14 a summary of the Pennsylvania State University Hartree-Fock relativistic code (PSUHFR) values of the charge density at the nucleus, $4\pi|\psi(0)|^2$, for each of Sb I configurations of interest here. In absence of Sb I isotope shift calculations (like those done by Aufmuth for other elements [49,50]) and particularly the scaling-factor value we are not able to use this equation directly except to compare the Sb I ratios of $a_{8s}^{10}(4p^2 8s)/a_{6s}^{10}(4p^2 6s) = 3.52/27.14 = 0.130$, $a_{7s}^{10}(4p^2 7s)/a_{6s}^{10}(4p^2 6s) = 8.05/27.14 = 0.297$, and $a_{5s}^{10}(5s 5p^4)/a_{6s}^{10}(4p^2 6s) = 414.38/27.14 = 15.26$. The agreement with corresponding ratios of the experimental values of Table 12 is very satisfactory for two first calculated ratios but rather worse for the last one, maybe because we did not exploit directly some experimental *A* hfs constants of the $5s 5p^4$ levels (not available up to now)

but only some bits existing in levels of other configurations (see index g in Tab. 7) when determining hfs single-electron parameters given in Table 12.

9 Conclusion

New Landé factors and hfs constants of 12 odd-parity and 6 even-parity levels of ^{123}Sb were determined experimentally. Using a linked-parameter technique of level-fitting calculations in a multiconfiguration basis a parametric analysis of fs structure involving in both cases of even and odd-parity levels up to seven configurations have been performed. The calculated g_J -factors deduced from the eigenvector compositions were compared with available experimental data and with ab initio Landé factor values computed by means of Cowan code. The agreements of the observed and calculated energy levels and g_J factors are very satisfactory.

Thanks to deduced eigenvectors, the expansions of hfs constants in intermediate coupling and extraction of mono-electronic parameter values semi-empirically were possible. Finally a complete list of the predicted hfs constants A of all levels of the studied system was generated.

The ab initio data computed by means of Cowan code for lowest configurations are highly similar to the experimental data. However it is known, that for high excited levels and Rydberg states the results of Cowan code are rather questionable and calculations should take into account second order perturbations, spin polarization and so on.

L.S. would like to thanks the University of Gdańsk for support by grant BW/538-5200-B869-15.

References

- D.M. Granty, R.K. Harris, *Encyclopedia of Nuclear Magnetic Resonance*, Vol. 5 (Wiley, Chichester, 1996)
- P. Raghavan, *At. Data Nucl. Data Tables* **42**, 189 (1989)
- W.F. Meggers, C.J. Humphreys, *J. Res. Nat. Bur. Stand.* **28**, 463 (1942)
- M. Hults, S. Mrozowski, *J. Opt. Soc. Am.* **54**, 855 (1964)
- S. Mrozowski, J. Czerwinska, R. Drozdowski, *J. Opt. Soc. Am.* **10**, 607 (1993)
- J.S. Badami, *Z. Phys.* **79**, 224 (1932)
- B. Buchholz, H.D. Kronfeld, G. Muller, M. Voss, R. Winkler, *Z. Phys. A* **288**, 247 (1978)
- F. Hassini, Z. Ben Ahmed, *J. Opt. Soc. Am. B* **5**, 2060 (1988)
- M. Voss, W. Weiss, B. Buchholz, R. Winkler, *Z. Phys. D* **1**, 151 (1986)
- M. Kopff, F. Les, B. Les, B. Malczyk, *Acta Phys. Pol.* **31**, 781 (1967)
- P.C.B. Fernando, G. Rochester, I.J. Spalging, K.F. Smith, *Phil. Mag.* **5**, 1291 (1960)
- A.A. Zaidi, Y. Makdisi, K.S. Bhatia, *J. Phys. B* **17**, 355 (1984)
- S. Werbowy, J. Kwela, *J. Phys. B* **43**, 065002 (2010)
- S. Werbowy, J. Kwela, *Phys. Rev. A* **77**, 023410 (2008)
- S. Werbowy, J. Kwela, *J. Phys. B* **42**, 065002 (2009)
- S. Werbowy, J. Kwela, *Can. J. Phys.* **87**, 851 (2009)
- T.J. Wąsowicz, R. Drozdowski, J. Kwela, *Phys. Scr.* **71**, 274 (2005)
- T.J. Wąsowicz, R. Drozdowski, J. Kwela, *Phys. Scr.* **72**, 200 (2005)
- T.J. Wąsowicz, R. Drozdowski, J. Kwela, *Eur. Phys. J. D* **36**, 249 (2005)
- L.M. Sobolewski, S. Werbowy, J. Kwela, *J. Opt. Soc. Am. B* **31**, 3038 (2014)
- S. Werbowy, J. Kwela, *Eur. Phys. J. ST.* **144**, 179 (2007)
- D. Grabowski, R. Drozdowski, J. Kwela, J. Heldt, *Z. Phys. D* **38**, 289 (1996)
- S. Werbowy, J. Kwela, R. Drozdowski, J. Heldt, *Eur. Phys. J. D* **39**, 5 (2006)
- S. Werbowy, J. Kwela, N. Anjum, H. Hühnermann, L. Windholz, *Phys. Rev. A* **90**, 032515 (2014)
- G. Müller, Dissertation, Technische Universität Berlin, 1974
- H. Hühnermann H, Dissertation, Philipps-Universität Marburg, Lahn, 1967
- J. Eisinger, G. Feher, *Phys. Rev.* **109**, 1172 (1958)
- M. Mazzoni, Y.N. Joshi, *Physica* **97C**, 107 (1979)
- Y.N. Joshi, V.N. Sarma, T.A.M. Van Kleef, *Physica* **125C**, 127 (1984)
- R. Beigang, J.J. Wynne, *J. Opt. Soc. Am. B* **3**, 949 (1986)
- J. Dembczyński, E. Stachowska, *Phys. Scr.* **43**, 248 (1991)
- S. Bouazza, H.O. Behrens, M. Fienhold, J. Dembczyński, G.H. Guthohrlein, *Eur. Phys. J. D* **6**, 311 (1999)
- S. Bouazza, P. Hannaford, M. Wilson, *J. Phys. B* **36**, 1537 (2003)
- S. Bouazza, *Phys. Scr.* **87**, 035303 (2013)
- S. Bouazza, *Phys. Scr.* **86**, 015302 (2012)
- S. Bouazza, R.A. Holt, D.S. Rosner, N.M.R. Armstrong, *J. Mod. Phys.* **5**, 511 (2014)
- R.D. Cowan, *The Theory of Atomic Structure and Spectra* (Berkeley, CA, University of California Press, 1981)
- S. Bouazza, R. Abjean, Y. Guern, 14th E.G.A.S. Conference, Liège, 1982
- C.E. Moore, *Nat. Bur. Standard* (1952)
- L.E. Howard, K.L.J. Andrew, *J. Opt. Soc. Am. B* **2**, 1032 (1985)
- J. Dembczyński, E. Stachowska, B. Arcimowicz, M. Bancewicz, *Physica C* **142**, 111 (1986)
- S. Bouazza, J. Bauche, J. Dembczyński, E. Stachowska, *Z. Phys. D* **7**, 185 (1987)
- P. Horodecki, J. Kwela, J.E. Sienkiewicz, *Eur. Phys. J. D* **6**, 435 (1999)
- S. Bouazza, M. Fienhold, G.H. Guthohrlein, H.O. Behrens, J. Dembczyński, *Eur. Phys. J. D* **6**, 303 (1999)
- S. Bouazza, J. Dembczyński, E. Stachowska, G. Szawiola, J. Ruczkowski, *Eur. Phys. J. D* **4**, 39 (1998)
- C. Schwartz, *Phys. Rev.* **51**, 380 (1955)
- S. Büttgenbach, *Hyperfine Interact.* **20**, 1 (1984)
- J. Dembczyński, W. Ertmer, U. Johan, P. Unkel, *Z. Phys. A* **321**, 1 (1985)
- P. Aufmuth, R. Kirsch A. Steudel, E. Wobker, *Z. Phys. D* **7**, 153 (1987)
- P. Aufmuth, I. Henneberg, A. Siminski, A. Steudel, *Z. Phys. D* **18**, 107 (1991)
- M. Wilson, *Physica C* **95**, 129 (1978)

Open Access This is an open access article distributed under the terms of the Creative Commons Attribution License (<http://creativecommons.org/licenses/by/4.0>), which permits unrestricted use, distribution, and reproduction in any medium, provided the original work is properly cited.